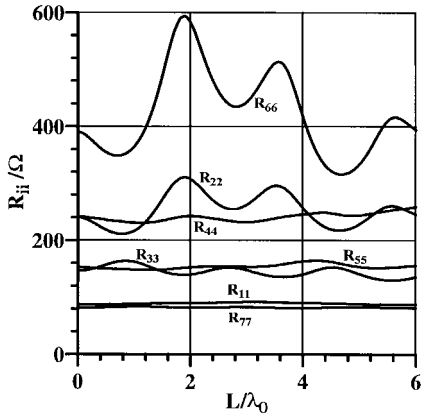

Fig. 5. Diagonal elements R_{ii} of optimal termination network under random excitation as a function of L/λ_0.

can be viewed as if the shorted line is part of the matching network required to minimize crosstalk between the remaining lines. However, on the other hand, if the shorted line is now excited, the termination is bound to fail. This fact supports our proposal for a termination network designed for random excitations.

The dependence of the total reflected power on the length of the transmission section, when a random voltage is incident at the generator, is shown in Fig. 4. The curve is periodic only if the modal propagation constants are commensurate. As an example of the dependence of the individual elements of the termination network on the line length, Fig. 5 shows the required variation of R_{11}, R_{22}, R_{33}, R_{44}, R_{55}, R_{66}, and R_{77} of the asymmetric seven-line structure in order to maintain optimum performance. It is interesting to note that the load element R_{66} is much more sensitive to the line length than the other resistances. Since all the excitations are assumed having equal probability, this effect is attributed to the fact that line number six is one of the narrowest (0.35 mm) with closest coupling distance (0.1 mm) to its immediate neighbors. Line number seven, although the narrowest, is immediately coupled only to line number six, and does not show as strong a sensitivity.

V. Conclusions

An analysis of the termination networks which lead to maximum power delivery, or minimum total reflected voltage, is presented for tightly coupled microstrip lines. Since an ideally matched matrix-type termination network can not be constructed, a termination network which minimizes the reflected power is designed instead. Even when the individual entries of the reflection matrix $[\rho_V]_{ij}$ are not small, it is possible to considerably reduce the reflected power or voltage by adjusting the phases and magnitudes of the individual reflected waves. Since the termination network which insures minimum power reflection depends on the nature of the incident excitation, the terminology *adaptive termination network* is arguably more appropriate. For unknown excitation, which is usually the case in practice, a termination network based on random excitation is proposed.

References

[1] K. D. Marx, "Propagation modes, equivalent circuits, and characteristic terminations for multiconductor transmission lines with inhomogeneous dielectrics," *IEEE Trans. Microwave Theory Tech.*, vol. MTT-21, pp. 450–457, July 1973.

[2] J. T. Kuo and C. K. C. Tzuang, "A termination scheme for high-speed pulse propagation on a system of tightly coupled coplanar strips," *IEEE Trans. Microwave Theory Tech.*, vol. 42, pp. 1008–1015, June 1994.

[3] G. T. Lei, G. W. Pan, and B. K. Gilbert, "Examination, clarification, and simplification of modal decoupling method for multiconductor transmission lines," *IEEE Trans. Microwave Theory Tech.*, vol. 43, pp. 2090–2100, Sept. 1995.

[4] T. Itoh, "Spectral domain immittance approach for dispersion characteristics of generalized printed transmission lines," *IEEE Trans. Microwave Theory Tech.*, vol. MTT-28, pp. 733–736, July 1980.

[5] D. Mirshekar-Syahkal, *Spectral Domain Method for Microwave Integrated Circuits.* New York: Wiley, 1990.

[6] S. Amari and J. Bornemann, "Non-perturbative fullwave analysis of lossy planar circuits," in *IEEE MTT-S Int. Microwave Symp. Dig.*, Orlando, FL, May 1995, pp. 1277–1280.

An FD–FD Formulation for the Analysis of the Optical Axis Misalignment Effect on Propagation Characteristics of Anisotropic Dielectric Waveguides

Carlos Leônidas da S. S. Sobrinho and Attílio J. Giarola

***Abstract*—A finite-difference frequency-domain (FD–FD) formulation is developed to study the dispersion characteristics of anisotropic dielectric waveguides with their optical axes not aligned with the coordinate-system axes. In this analysis, the optical axes are initially assumed to be aligned with the coordinate-system axes such that the electric-permittivity and magnetic-permeability tensors are diagonal. The optical axes of the anisotropic dielectric are then rotated an angle θ (or ϕ) with respect to the coordinate-system axes. While the FD–FD formulation developed is general, it is applied here only to waveguides containing uniaxial anisotropic dielectrics. The results show that accurate optical-axis orientation is important in the design of dielectric waveguides.**

***Index Terms*—Optical axial misalignment.**

I. Introduction

Various methods have been used in the analysis of the propagation characteristics of dielectric waveguides, with applications in integrated circuits in the millimeter and optical frequency bands. Among these methods, the following are of interest:

1) the finite-difference frequency-domain (FD–FD) formulation [1], [2];
2) the two-dimensional (2-D) finite-difference time-domain (2-D FDTD) method [3];
3) the finite-element method (FEM) [4];
4) the transmission-line method (TLM) [5].

While the FD–FD, FEM, and TLM in the frequency-domain methods are equivalent, this is not true for the FD–FD and 2-D

Manuscript received December 12, 1995; revised June 20, 1997. This work was supported in part by the Brazilian agencies CNPq, TELEBRÁS, FINEP, and CAPES.

C. L. da S. S. Sobrinho is with the Electrical Engineering Department, Federal University of Pará (UFPa), Belém, PA, Brazil 66075-900.

A. J. Giarola is with the School of Electrical Engineering, State University of Campinas (UNICAMP), Campinas, SP, Brazil, 13083-970.

Publisher Item Identifier S 0018-9480(97)07118-4.

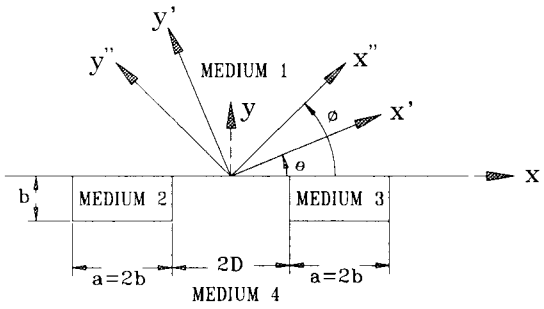

Fig. 1. Waveguide structure.

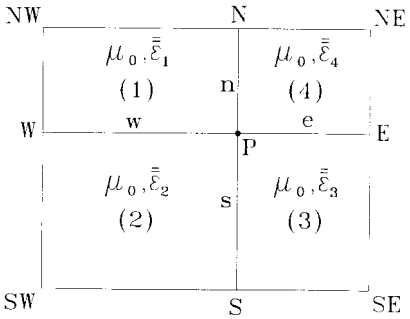

Fig. 2. Graded mesh with five and nine points.

FDTD methods. There are some basic differences, such as for the same computation time, the 2-D FDTD method allows a more precise definition of the field distribution, particularly at the interfaces. However, for the analysis of waveguides containing dispersion materials, contrary to the FD–FD method, the 2-D FDTD method does not allow the calculation of the attenuation constant with adequate precision. Considering this fact and the mathematical development simplicity of its implementation, we have chosen to develop a formulation using the FD–FD method that is an extension of [2].

II. Theory

The formulation developed in this paper is applicable to the analysis of the propagation characteristics of cylindrical waveguides with arbitrary cross section, consisting of general biaxial anisotropic lossy dielectrics, with their optical axes not necessarily aligned with the coordinate axes.

Fig. 1 shows a cross section of the structure considered here. Media 2 and 3 are channel waveguides integrated in a substrate denominated as Medium 4. The envelope is Medium 1. In the general formulation that was developed, all four media are characterized by the following dielectric permittivity and magnetic permeability tensors:

$$\bar{\bar{\varepsilon}} = \varepsilon_0 \begin{bmatrix} \varepsilon_{xx} & \varepsilon_{xy} & 0 \\ \varepsilon_{yx} & \varepsilon_{yy} & 0 \\ 0 & 0 & \varepsilon_{zz} \end{bmatrix} \text{ and } \bar{\bar{\mu}} = \mu_0 \begin{bmatrix} \mu_{xx} & \mu_{xy} & 0 \\ \mu_{yx} & \mu_{yy} & 0 \\ 0 & 0 & \mu_{zz} \end{bmatrix} \tag{1}$$

respectively, where ε_0 and μ_0 are the free-space permittivity and permeability, respectively. They result from a rotation in the z-axis of an angle θ with respect to the x-axis, for the dielectric permittivity and an angle ϕ with respect to the x-axis for the magnetic permeability, from the aligned axes position

$$\begin{aligned} \tau_{xx} &= \tau_2 \sin^2(\delta) + \tau_1 \cos^2(\delta) \\ \tau_{yy} &= \tau_2 \cos^2(\delta) + \tau_1 \sin^2(\delta) \\ \tau_{zz} &= \tau_3 \quad \tau_{xy} = \tau_{yx} = (\tau_2 - \tau_1) \sin(\delta) \cos(\delta) \end{aligned} \tag{2}$$

where $\delta = \theta$ when $\tau = \varepsilon$ and $\delta = \phi$ when $\tau = \mu$. The angles θ and ϕ are shown in Fig. 1. The fields are assumed to have a harmonic time dependence given by $\exp(\mathrm{j}\omega \mathrm{t})$ and propagating along the z-direction (see Fig. 1), with a z-dependence of the form $\exp(-\gamma_z z)$, where ω is the angular frequency and γ_z is the propagation constant.

For the bi-dimensional problem, the vector wave equation that describes the wave propagation, is expressed in terms of the transverse components of the magnetic field in the waveguide cross section (Fig. 1). As a result, two coupled partial differential equations are obtained and written as follows:

$$\begin{aligned} 0 = {} & p\frac{\partial^2 H_\alpha}{\partial \alpha^2} + q\frac{\partial^2 H_\alpha}{\partial \tau^2} + r\frac{\partial^2 H_\alpha}{\partial \alpha \partial \tau} - t\frac{\partial^2 H_\tau}{\partial \alpha^2} + u\frac{\partial^2 H_\tau}{\partial \tau^2} \\ & + v\frac{\partial^2 H_\tau}{\partial \alpha \partial \tau} + H_\alpha + F\gamma_z^2 H_\alpha + G\gamma_z^2 H_\tau \end{aligned} \tag{3a}$$

where $\alpha = x$ when $\tau = y$ and $\alpha = y$ when $\tau = x$

$$\begin{aligned} & p = \frac{V_1 \mu_{\alpha\alpha} L}{\mu_{zz}} \quad u = V_2 L \frac{\mu_{\tau\tau}}{\mu_{zz}} \quad q = L\left(\frac{V_2 \mu_{\tau\alpha}}{\mu_{zz}} + \frac{\mu_{\tau\tau}}{\varepsilon_{zz}}\right) \\ & v = L\left(V_2 \frac{\mu_{\alpha\tau}}{\mu_{zz}} + V_1 \frac{\mu_{\tau\tau}}{\mu_{zz}} - \frac{\mu_{\tau\tau}}{\varepsilon_{zz}}\right) \\ & r = L\left(V_2 \frac{\mu_{\alpha\alpha}}{\mu_{zz}} + V_1 \frac{\mu_{\tau\alpha}}{\mu_{zz}} + \frac{\mu_{\alpha\tau}}{\varepsilon_{zz}}\right) \\ & F = LV_1 \quad t = L\left(\frac{\mu_{\alpha\tau}}{\varepsilon_{zz}} - V_1 \frac{\mu_{\alpha\tau}}{\mu_{zz}}\right) \quad G = LV_2 \\ & L = \frac{-1}{\omega^2 D} \quad D = \mu_{\tau\alpha}\mu_{\alpha\tau} - \mu_{\tau\tau}\mu_{\alpha\alpha} \quad V_2 \frac{\mu_{\tau\alpha}\varepsilon_{\alpha\alpha} - \mu_{\alpha\alpha}\varepsilon_{\alpha\tau}}{E} \\ & V_1 = \frac{\mu_{\tau\alpha}\varepsilon_{\tau\alpha} - \mu_{\alpha\alpha}\varepsilon_{\tau\tau}}{E} \quad E = \varepsilon_{\tau\alpha}\varepsilon_{\alpha\tau} - \varepsilon_{\tau\tau}\varepsilon_{\alpha\alpha}. \end{aligned} \tag{3b}$$

A. Numerical Solution of Coupled Equations (3a)

To develop the finite-difference method, a graded mesh of points is drawn on the waveguide cross section, such that a general point P_i is distant from its neighbors to east, west, south, and north by e, w, s, and n, respectively, as shown in Fig. 2. To obtain the H_x and H_y components of the magnetic field in a position P_i, the coupled equations (3a) are applied to each region 1–4 of the nine points graded mesh of Fig. 2. The first- and second-order partial derivatives of the transverse components of the magnetic field H_x and H_y are obtained from a truncated Taylor series for the respective mesh points (Fig. 2). As a result, eight equations are obtained. In the interfaces between the four regions of the nine-point graded mesh of Fig. 2, the boundary condition that requires continuity of longitudinal electric E_z and magnetic H_z field components is imposed [2].

The solution of the wave equation may, therefore, be written for a point P, as

$$\begin{aligned} -\gamma_z^2 H_{yp} = {} & \sum_{i=W,E,N,S} D^i H_{xi} + \sum_{i=W,E,N,S} C^i H_{yi} \\ & + \sum_{k=NW,SW,NE,SE} D^k H_{xk} + \\ & + \sum_{k=NW,SW,NE,SE} C^k H_{yk} + D^p H_{xp} + C^p H_{yp} \end{aligned} \tag{4a}$$

$$\begin{aligned} -\gamma_z^2 H_{xp} = {} & \sum_{i=W,E,N,S} A^i H_{xi} + \sum_{i=W,E,N,S} B^i H_{yi} \\ & + \sum_{k=NW,SW,NE,SE} A^k H_{xk} + \\ & + \sum_{k=NW,SW,NE,SE} B^k H_{yk} + A^p H_{xp} + B^p H_{yp}. \end{aligned} \tag{4b}$$

The coefficients that appear in (4a) and (4b) are functions of geometry and electromagnetic parameters of the structure under analysis.

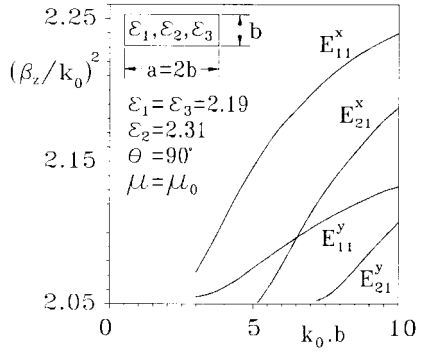

Fig. 3. Dispersion characteristics of first four E^x_{pq} and E^y_{pq} modes for the isolated waveguide.

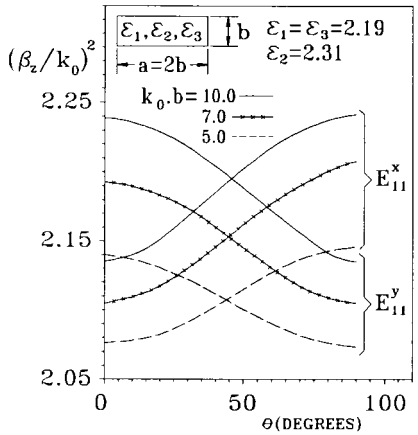

Fig. 4. Effective dielectric constant $(\beta_z/k_0)^2$ of E^x_{11} and E^y_{11} modes as a function of θ for the waveguide of Fig. 3.

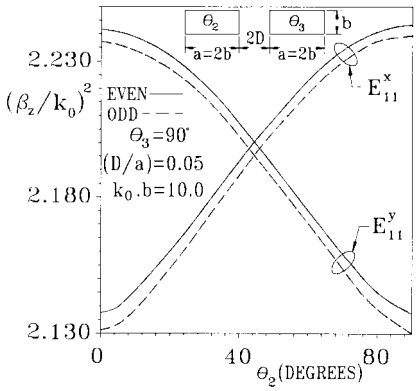

Fig. 5. Effective dielectric constant $(\beta_z/k_0)^2$ of even and odd E^x_{11} and E^y_{11} modes as a function of θ_2 for the coupled waveguides of Fig. 1.

B. Limitation of the Discretization Region

The graded mesh of points is assumed to have N points. Therefore, there are N unknowns H_{yp} and N unknowns H_{xp}. Using (4a) and (4b) for each mesh point, $2N$ equations are obtained. Therefore, the number of unknowns is equal to the number of equations. Obviously, to solve the problem, N has to be a finite number. This is done by confining the structure's cross section within electric and/or magnetic walls. The use of the present formulation in open structures is possible when the fields are concentrated near the center of the cross section (Media 2 and 3 of Fig. 1) due to the high dielectric permittivity of these media when compared with the other media (Media 1 and 4 of Fig. 1). In these situations, the influence of the walls on the results may be controlled [1], [2].

As a result, (4a) and (4b) may be applied to each point P of the graded mesh of points using the proper boundary conditions at the electric and/or magnetic walls. Therefore, a system of homogeneous and linear equations is obtained that may be written as a conventional eigenvalue problem [1]

$$[(A) - \lambda(U)]\,(X) = 0 \tag{5}$$

where $\lambda = -\gamma_z^2$, (U) is the unit matrix, (X) is a column matrix that contains the components of the magnetic field H_x and H_y, and (A) is a square matrix with constant coefficients. The values of the attenuation constant α_z and phase constant β_z of each propagation mode are obtained from each eigenvalue by means of

$$\lambda = -(\alpha_z + j\,\beta_z)^2. \tag{6}$$

The eigenvalues λ and the eigenvectors (X) were obtained using the Eispack program.

III. Results

The developed formulation is applied to the analysis of the dispersion characteristics of the structure considered in Fig. 1. In this analysis, the magnetic permeability of all four media are assumed to be equal to that of free-space $\overline{\overline{\mu}} = \mu_0$. Media 1 and 4 are assumed to be isotropic, with $\overline{\overline{\varepsilon}}/\varepsilon_0 = 2.05$, and Media 2 and 3 are assumed to be uniaxial anisotropic dielectrics, with $\varepsilon_1 = \varepsilon_3 = 2.19$ and $\varepsilon_2 = 2.31$ (2). The free-space wavenumber is given by $k_0 = \omega\sqrt{\mu_0\varepsilon_0}$ and the aspect ratio of each waveguide is $(a/b) = 2$.

Fig. 3 shows the dispersion characteristics of the first four E^x_{pq} and E^y_{pq} modes, for the case of an isolated waveguide ($D \gg a$). An angle $\theta = 90^\circ$ was used. Because of the structure's symmetry, only one fourth of its cross section was sufficient for the present analysis. A 13×13 graded mesh of points was used. The results shown here were compared with those obtained using a vector FEM and a good agreement was observed.

The dispersion characteristics for the isolated waveguide examined in Fig. 3 are shown in Fig. 4, as a function of the angle θ, for the E^x_{11} and E^y_{11} modes and for three different normalized frequencies $k_0 b = 5.0$, 7.0, and 10.0. Note that the effective dielectric constant $(\beta_z/k_0)^2$ versus θ is very smooth.

In Fig. 5, coupled dielectric waveguides are considered. The angle θ_3 for Medium 3 is kept constant and equal to 90°, while the angle θ_2 for Medium 2 is varied. A graded mesh of 13 points by 49 points was used in this case and advantage was taken of the structure's symmetry with respect to the x-axis. Curves for $(\beta_z/k_0)^2$ versus θ_2 for the even and odd E^x_{11} and E^y_{11} modes are shown for $k_0 b = 10.0$. Note that while $(\beta_z/k_0)^2$ varies with θ_2, the differences of $(\beta_z/k_0)^2$ between even and odd modes is practically independent of θ_2.

IV. Conclusions

An FD–FD method was formulated for the analysis of cylindrical biaxial anisotropic dielectric waveguides with their optical axes rotated with respect to the coordinate system axes.

The formulation was developed in terms of the transverse magnetic-field components such that the problem was transformed into a conventional eigenvalue problem, with the elimination of the spurious modes by the implicit inclusion of the divergence of the magnetic field equal to zero.

Various results for the effective dielectric constant were presented for isolated and coupled waveguides. In all cases considered here, particular attention was taken to the effect caused by the rotation of the material optical axes in a plane transverse to the direction of

propagation, with the indication that it cannot be ignored. For the case of coupled waveguides, it was noted that the coupling is practically unaffected when the optical axes of one of the waveguides are rotated with respect to the coordinate-system axes.

REFERENCES

[1] N. Schulz, K. Bierwirth, and F. Arndt, "Finite-difference analysis of integrated optical waveguides without spurious mode solutions," *Electron. Lett.*, vol. 22, no. 18, pp. 963–965, Aug. 1986.

[2] C. L. da S. S. Sobrinho and A. J. Giarola, "Analysis of an infinite array of rectangular anisotropic dielectric waveguides using the finite-difference method," *IEEE Trans. Microwave Theory Tech.*, vol. 40, pp. 1021–1025, May 1992.

[3] S. Xiao and R. Vahldieck, "An efficient 2-D FDTD algorithm using real values," *IEEE Microwave Guided Wave Lett.*, vol. 3, pp. 127–129, May 1993.

[4] K. Hayata, M. Koshiba, M. Eguchi, and M. Suzuki, "Vectorial finite-element method without any spurious solutions for dielectric waveguiding problems using transverse magnetic-field component," *IEEE Trans. Microwave Theory Tech.*, vol. MTT-34, pp. 1120–1124, Nov. 1986.

[5] J. Huang and K. Wu, "Toward a generalized TLM algorithm for solving arbitrary reciprocal and nonreciprocal planar structures," *IEEE Trans. Microwave Theory Tech.*, vol. 44, pp. 1508–1511, Aug. 1996.

Scattering by an Infinite Elliptic Dielectric Cylinder Coating Eccentrically a Circular Metallic or Dielectric Cylinder

Stylianos P. Savaidis and John A. Roumeliotis

***Abstract*—In this paper, the scattering of a plane electromagnetic wave by an infinite elliptic dielectric cylinder, coating eccentrically a circular metallic or dielectric inner cylinder, is treated. The electromagnetic field is expressed in terms of both circular and elliptical–cylindrical wave functions, which are connected with one another by well-known expansion formulas. Translational addition theorems for circular cylindrical wave functions are also used. If the solution is specialized to small values of $h = k_2 c/2$, where k_2 is the wavenumber of the elliptic dielectric cylinder and c its interfocal distance, semianalytical expressions of the form $S(h) = S(0)[1 + gh^2 + O(h^4)]$ are obtained for the scattered field and the various scattering cross sections of this configuration. The coefficients g are independent of h. Both polarizations are considered for normal incidence. Graphical results for the scattering cross sections are given for various values of the parameters.**

***Index Terms*—Eccentric elliptical–circular cylinders, scattering.**

I. INTRODUCTION

Scattering from composite bodies is often used for detecting their internal structure. Analytical solution of such problems is severely limited by the shape of boundaries. For complicated geometries, various numerical methods can be used.

Scattering from a dielectric elliptic cylinder coated with another nonconfocal dielectric one, or from two parallel dielectric elliptic cylinders, is examined in [1] and [2], respectively.

In this paper, the scattering of an electromagnetic plane wave by an infinite elliptic dielectric cylinder containing an off-axis metallic or dielectric circular inner cylinder, is considered. The geometry of the scatterer, shown in Fig. 1, is a perturbation of the eccentric circular one, with radii R_1 and R_2. All materials are lossless. Both polarizations are considered for normal incidence.

Using translational addition theorems for circular cylindrical wave functions [3] and expansion formulas between circular and elliptical (Mathieu) wave functions [3], [4], we conclude (after the satisfaction of the boundary conditions and some manipulation) with two infinite sets of linear nonhomogeneous equations for the expansion coefficients of the electromagnetic field inside the elliptic dielectric cylinder.

For general values of $h = k_2 c/2$ these sets can be only solved numerically by truncation, but for $h \ll 1$, a semianalytical solution is possible. After very lengthy and laborious, but straightforward calculations, we obtain expressions of the form $S(h) = S(0)[1 + gh^2 + O(h^4)]$ for the scattered field and the scattering cross sections. The coefficients g are independent of h, while $S(0)$ corresponds to the eccentric circular problem. The main advantage is that these expressions are valid for each small h, *free* of Mathieu functions, while all purely numerical techniques require repetition of the calculation for each different h, a very complicated task due to these functions.

This advantage distinguishes this paper from [1], [5], which contribute more general geometries. By using the solutions of [1] and [5] to obtain our numerical results, one should repeat the very complicated steps containing the calculation of the various Mathieu functions for each different h.

Apart from its mathematical interest, the elliptical–circular combination of this problem may enhance or decrease the various scattering cross sections, as compared to those for the eccentric circular geometry.

The solution of this problem is much more complex and lengthy than that in the corresponding coaxial one [6] due to the eccentricity, the presence of a dielectric inner cylinder in one case here, and the use of different permeabilities for the various regions in this paper. In [6], the wavenumbers in the elliptic dielectric cylinder and the surrounding medium were also nearly equal ($h \cong h_2$ there), while here they are different.

II. METALLIC INNER CYLINDER

A. E-Wave Polarization

1) Calculation of the Field: We begin with a metallic inner cylinder and the E-wave polarization. The incident plane wave normally impinging on the z-axis has the form [3], [4]

$$E_z^{inc} = \sqrt{8\pi} \sum_{m=0}^{\infty} j^{-m} \left[\frac{Se_m(h_3, \cos\psi)}{M_m^e(h_3)} \times Se_m(h_3, \cos\theta) Je_m(h_3, \cosh\mu) + \frac{So_m(h_3, \cos\psi)}{M_m^o(h_3)} So_m(h_3, \cos\theta) \times Jo_m(h_3, \cosh\mu) \right], \qquad h_3 = \frac{k_3 c}{2} \quad (1)$$

with μ, θ the transverse elliptical–cylindrical coordinates with respect to xOy, $Je_m(Jo_m)$ the even (odd) radial Mathieu functions of the first kind, and $Se_m(So_m)$ the even (odd) angular Mathieu functions. The normalization constants $M_m^{e(o)}$ are given in [4]. The angle ψ defines the direction of incidence with respect to x. The time dependence $\exp(j\omega t)$ is suppressed throughout.

Manuscript received January 23, 1996; revised June 20, 1997.

The authors are with the Department of Electrical and Computer Engineering, National Technical University of Athens, Athens 15773, Greece.

Publisher Item Identifier S 0018-9480(97)07114-7.